

Summer Programs Symposium

July 31st – August 1st, 2024



Abstract Booklet

Summer Program for Undergraduate Research (SPUR)

Radhika Ramesh – University of Wisconsin at Parkside
Kajana Satkunendrarajah, PhD
MCW Department of Neuroscience

Disruption of Forelimb Neural Networks in Degenerative Cervical Myelopathy

A leading non-traumatic spinal cord injury known as degenerative cervical myelopathy (DCM), is characterized by chronic compression of the cervical spinal cord which leads to substantial spinal cord dysfunction. The most common cause for chronic compression is cervical spinal stenosis caused by gradual age-related degradation and ossification of ligaments surrounding the cervical spinal cord. Patients typically experience varying types of motor dysfunction including deficits in their hands, impaired gait and balance, pain, and sensory disturbances. Among these symptoms, hand and upper limb function impairments are particularly debilitating as they directly affect patients' independence and quality of life (Nouri et al., 2015). Currently there are no effective strategies to enhance the upper arm disfunction in DCM patients, apart from decompression surgery. Despite surgical decompression being the primary treatment, over 30% of patients fail to achieve significant clinical recovery post-surgery, and more than 40% continue to suffer from considerable residual disability (Evaniew et al., 2020; Tetreault et al., 2016; Karadimas et al., 2015). Furthermore, current research lacks a comprehensive understanding of neural circuit changes related to forearm function in DCM. One of the barriers to advancing the pathophysiology of DCM is the sparsity of animal models of DCM. This study hypothesizes that DCM forelimb deficits are due to the loss of neural networks in the cervical spinal cord and their descending input from brainstem neurons. Using a clinically relevant mouse model of DCM, we assessed forelimb related motor function in the chronic phase of DCM performed a detailed anatomical characterization of the forelimb neural circuitry using a retrograde transneuronal viral tracing strategy. Horizontal ladder walk and grip strength behavioral assessments revealed significant forelimb deficits in DCM akin to that seen in DCM patients. Furthermore, our findings reveal significant reduction in motor neurons and interneurons in the spinal cord (C1-T4) and a marked decrease in supraspinal brainstem neurons modulating forelimb function in DCM mice compared to control. In conclusion, this study provides the first anatomical map of the spinal and supraspinal networks controlling forelimb muscles in DCM, providing a foundation for future research to improve functional recovery in DCM patients.

Keywords: Degenerative Cervical Myelopathy, Spinal Cord Injury, Upper limb, Impairment, Forelimb Motor Dysfunction, Neural Degeneration, Motor Neurons, Interneurons

Citations

- Card, J. P., & Enquist, L. W. (2001). Transneuronal circuit analysis with pseudorabies viruses. *Current protocols in neuroscience*, Chapter 1, Unit 1.5. <https://doi.org/10.1002/0471142301.ns0105s09>
- Hendelman, W. J., Humphreys, P., & Skinner, C. (2009). *Integrated Nervous System: A Systematic Diagnostic Approach*. CRC Press.
- Kalsi-Ryan, S., Riehm, L. E., Tetreault, L., Martin, A. R., Teoderascu, F., Massicotte, E., Curt, A., Verrier, M. C., Velstra, I. M., & Fehlings, M. G. (2020). Characteristics of Upper Limb Impairment Related to Degenerative Cervical Myelopathy: Development of a Sensitive Hand Assessment (Graded Redefined Assessment of Strength, Sensibility, and Prehension Version Myelopathy). *Neurosurgery*, 86(3), E292–E299. <https://doi.org/10.1093/neuros/nyz499>
- Karadimas, S. K., Satkunendrarajah, K., Laliberte, A. M., Ringuette, D., Weisspapir, I., Li, L., Gosgnach, S., & Fehlings, M. G. (2019). Sensory cortical control of movement. *Nature Neuroscience*, 23(1), 75–84. <https://doi.org/10.1038/s41593-019-0536-7>
- Metz, G. A., & Whishaw, I. Q. (2009). The ladder rung walking task: a scoring system and its practical application. *Journal of visualized experiments : JoVE*, (28), 1204. <https://doi.org/10.3791/1204>
- Satkunendrarajah, K., Karadimas, S. K., Laliberte, A. M., Montandon, G., & Fehlings, M. G. (2018). Cervical excitatory neurons sustain breathing after spinal cord injury. *Nature*, 562(7727), 419–422. <https://doi.org/10.1038/s41586-018-0595-z>
- Sweetman, H., Rahman, M., Vedantam, A., & Satkunendrarajah, K. (2024). Subclinical respiratory dysfunction and impaired ventilatory adaptation in degenerative cervical myelopathy. *Experimental Neurology*, 371, 114600. <https://doi.org/10.1016/j.expneurol.2023.114600>
- Takeshita, H., Yamamoto, K., Nozato, S., Inagaki, T., Tsuchimochi, H., Shirai, M., Yamamoto, R., Imaizumi, Y., Hongyo, K., Yokoyama, S., Takeda, M., Oguro, R., Takami, Y., Itoh, N., Takeya, Y., Sugimoto, K., Fukada, S., & Rakugi, H. (2017b). Modified forelimb grip strength test detects aging-associated physiological decline in skeletal muscle function in male mice. *Scientific Reports*, 7(1). <https://doi.org/10.1038/srep42323>
- Wilcox, J.T., et al., Generating level-dependent models of cervical and thoracic spinal cord injury: Exploring the interplay of neuroanatomy, physiology, and function. *Neurobiol Dis*, 2017. 105: p. 194-212.

The Effect of Music Predictability on Respiratory Rhythm in Mice

Music can synchronize brain dynamics, influencing emotional, cognitive, and physical states. The exact neurological benefits remain unknown due to the complexity of music, especially Western classical music, but it is known that neurons can synchronize to rhythmic stimuli. Recently, it has been demonstrated that the primary sensory cortex (SI), a brain region responsible for higher-order sensory processing, exerts an efferent motor control (locomotion). These neurons have also been shown to receive input from the auditory cortex. Given that musical rhythms can entrain neurons, we hypothesize that auditory stimuli, such as classical music, could modulate respiratory rhythms via neural connectivity between the auditory cortex, primary somatosensory cortex, and brainstem respiratory centers. To test this, mice were exposed to four different auditory stimuli – counterbalanced for each trial – with variable β , a measure of rhythmic predictability where higher β value indicates more predictable rhythm. During musical exposure to ambient noise (room noise), white noise ($\beta=0$), Sonata for Two Pianos in D Major K.448 ($\beta=0.6$), and Fur Elise ($\beta=1.2$), respiratory rhythm data was collected via whole-body plethysmography. Data revealed that breathing frequency increases with the rhythmic complexity of musical pieces, following the Yerkes-Dodson inverted U pattern and suggesting a complex interaction between music and respiratory rhythm. In parallel, we investigated the anatomical relationships between the diaphragm and primary somatosensory cortex using retrograde trans-neuronal viral tracing. These results demonstrated that the primary somatosensory cortex, which receives direct input from the auditory cortex, is anatomically connected to rhythm-generating neural networks in the brainstem and phrenic motoneurons that innervate the diaphragm, the main inspiratory muscle. Our findings suggest a correlation between Western classical music's rhythmic intricacies and mice's breathing frequency. The anatomical basis for this relationship appears to involve connectivity between the brainstem and spinal cord regions responsible for respiratory rhythm generation and the primary somatosensory cortex. These results lay the ground work to future research of how music can positively impact health, and how music may be used as a more accessible and non-invasive enhancement to respiratory therapies.

Keywords: Primary somatosensory cortex, auditory cortex, diaphragm, breathing, neuron entrainment, retrograde transsynaptic viral tracing, rhythm-generating neural networks

Alexander Drobek – Milwaukee School of Engineering
L. Tugan Muftuler, PhD
MCW Department of Neurosurgery

Pyradiomics Analysis: A New Approach to Understanding Chronic Low Back Pain

Background

Chronic low back pain (cLBP) affects over 600 million people worldwide, with unknown direct causes. Current clinical techniques are time-consuming and inadequate for personalized medicine. Previous work has shown that pathologic changes in vertebral endplates are strongly associated with pain symptoms. PyRadiomics is an open-source Python package for radiomic feature extraction from medical imaging.

Method

We analyzed 53 subjects with DCE-MRI scans of the lumbar spine. Using PyRadiomics, we extracted 48 shape and size metrics from perfusion maps. Vertebral endplate masks generated 2D projections of perfusion. A synthetic dataset was created from 9 endplates with smooth perfusion, resulting in over 30,000 entries. Lesions were added in varying sizes, locations, and types, classified into 7 classes. XGBoost, MLP, and ResNet-based approaches were used as classifiers.

Results

Hyperparameter optimization yielded stable, accurate models on holdout data sets. The highest performing XGBoost model achieved $97.8 \pm 0.03\%$ test accuracy, while the highest performing MLP and ResNet-based models achieved $96.0 \pm 0.05\%$ and $95.7 \pm 0.04\%$ test accuracy, respectively. However, classification on the unlabeled "real" dataset revealed that the synthetic data was not representative enough of real data, highlighting the need for more diverse and realistic synthetic data or the use of real data for training. The models struggled to generalize to the real dataset, indicating a gap between the synthetic and real data distributions.

Conclusion

This novel method shows promise for studying chronic low back pain. PyRadiomics is more robust than raw image data for lesion identification with endplate perfusion maps, allowing for smaller models and less compute usage while yielding more stable and higher performing results. Endplate lesion classification would be beneficial for further endplate perfusion study.

Kale Kroenke, Rowan University
Stéphanie Van-Stichelen, PhD
MCW Department of Biochemistry

Developing CRISPR/Cas9 Knockout Cell Lines for Sucralose Drug Efflux Inhibition

Background: Over the past few decades, consumption of non-nutritive sweeteners (NNS) in the United States has significantly increased. Several studies and previous research in our lab have identified the non-nutritive sweetener sucralose (brand name Splenda), as a substrate for P-Glycoprotein (PGP). PGP is a multidrug efflux transporter whose substrates include antibiotics, antivirals, antiarrhythmics, antidepressants and chemotherapeutics. We hypothesize that sucralose acts as a competitive inhibitor for PGP. This would suggest sucralose consumption could interfere with effective detoxification, impacting dose, distribution, and duration of drugs in the body. Previous work measured the viability of Hek293T cells co-treated with sucralose and chemotherapeutic Doxorubicin and indicated that the addition of sucralose increases accumulation of intracellular drug exposure, leading to higher rates of cell death. However, while Hek293T cells do have high endogenous expression of PGP, they also express lower levels of other drug efflux proteins, including BCRP, which can also efflux Doxorubicin. To be able to validate specificity of Doxorubicin accumulation to PGP inhibition by sucralose, CRISPR/Cas9 *ABCB1* (encodes PGP) knockout cell lines were developed for future experimental use.

Methods: Three single-guide RNAs (sgRNAs) were developed that matched segments of exon 11 in the *ABCB1* gene. All sgRNAs were mixed and complexed with the Cas9 enzyme and transfected into Hek293T cells starved in serum-free DMEM for 3h prior. Cells were grown in a 24 well plate for 72h before validation and quantification of transfection efficiency using PCR and qPCR, after which they were harvested and diluted to 1 cell/well in a 96 well plate for clonal expansion. Cells in the 96 well plates were counted daily to ensure monoclonal populations were present for 2 weeks before passage into a 24 well plate for continued growth and maintenance.

Results: qPCR analysis revealed 25% of the Hek293T cell population exhibited a successful *ABCB1* knockout. Distinct differences in morphology and proliferation were observed during clonal selection between WT Hek293T cells and *ABCB1* KO Hek293T cells.

Conclusion and future directions: This work demonstrated that successful knockout of the *ABCB1* gene (PGP) is possible in the Hek293T line, however it may affect the viability, proliferation, and morphology of the cells. Steps must be taken to ensure effective clonal expansion, including but not limited to adding serum or amino acids to media to promote growth and more frequent passage. Additionally, PCR and Sanger sequencing of PCR product must be conducted to confirm *ABCB1* knockout and identity of gene mutations in monoclonal populations. If expansion of monoclonal populations to viable cell lines is unsuccessful, developing sgRNAs that target a different PGP exon may improve both transfection and proliferation efficiency. In the future, this stable cell line will be used for further inquiry into previous sucralose/chemotherapeutic co-treatment work and interactions of other non-nutritive sweeteners with PGP. We will expand this process into other cells lines used in drug efflux research and generate multiple drug efflux transporter KO.

Keywords: Non-nutritive sweeteners, CRISPR/Cas9, Sucralose, PGP, Multi-drug efflux transporters

Candice Tacconi – University of Lille, France
Stéphanie Olivier-Van Stichelen, PhD
MCW Department of Biochemistry

Hormone-related proteins are differentially *O*-GlcNAc-modified in male vs. female and healthy vs. GDM placentas.

Background

Gestational diabetes Mellitus (GDM) is characterized by elevated blood glucose levels during pregnancy due to the body's resistance to the action of insulin. For some women, the pancreas cannot produce enough insulin, leading to hyperglycemia, causing GDM. For most, GDM resolve after delivery, which suggest a placental origin for GDM. The consequences of GDM are risks of maternal-fetal complications for the mother and for the fetus, an increased risk of having diabetes later in life. *O*-GlcNAcylation is an abundant post-translation modification of proteins. It is the addition of a single GlcNAc molecule to serine or threonine residues on proteins through an *O*-linked β -glycosidic bond. The addition of GlcNAc is catalyzed by OGT (*O*-GlcNAc transferase), and the cleavage is catalyzed by OGA (*O*-GlcNAcase). Interestingly, the deregulation of *O*-GlcNAcylation is closely linked to GDM. Placental *OGT* and *OGA* expression levels differ in healthy or GDM patients, and *OGT* impacts the expression of key hormones in the placenta. Previous work in the lab also highlighted some sex-specific *O*-GlcNAc placental dysfunctions in GDM, which correlates with statistics showing that carrying a male fetus increases the risk of GDM compared to a female. Additionally, *OGT* is located on the X-chromosome, and is thought to escape X inactivation in specific settings.

Thus we *hypothesize that proteins are differentially O-GlcNAcylated in Healthy and GDM in a sex specific manner*. To test this hypothesis, we performed an *O*-GlcNAcomic experiments by mass spectrometry and identified differentially *O*-GlcNAcylated protein in male, female, Healthy and GDM human placentas. In the current study, we would like to validate the variation of *O*-GlcNAcylation on the previously identified proteins by WB (Western-Blot).

Method

Previously, banked placentas (n=40) were obtained from male and female fetuses and mothers with GDM or healthy pregnancies. Proteins from each placenta sample were extracted, and the extracts were analyzed by MS. This data allowed for the creation of a repository of proteins differentially *O*-GlcNAcylated in Healthy vs. GDM, and Male vs. Female placentas.

For this, we first used model cell lines to verify the suitability of the antibodies for each protein by Western-Blot, so we could later reproduce it in the placenta samples. Cell lines included Hek293T, BeWo, and HeLa, which come respectively from the kidney, placenta, and cervical tissues. We chose those cell lines because they had the best demonstrated affinity for our antibodies. A total of 6 proteins were analyzed with the cell lines: DCP1A, ATXN2L, CAPS1, TCF12, IRS4, and NAV3.

Results

The optimal conditions for WB were the following: 8% Tris-Glycine gel, 5% BSA (Bovine Serum Albumin) for blocking and primary antibody dilution, 5% methanol transfer buffer, ponceau, and HRP (Horseradish Peroxidase) secondary antibodies. Of the 6 proteins, 2 were successfully detected in HeLa,

4 in BeWo, and 5 in HEK293T cells. However, only 1 (ATXN2L) was detected in human placental total protein extracts.

Conclusion

This first verification validated the presence of 5 proteins in cell lines and 1 in human tissue sample: ATXN2L. The presence of the proteins in cell lines and not in human tissue is likely caused by the higher contamination of blood proteins, which led to loss of band definition on WB.

The next step will involve cleaning the samples of blood proteins by using the “Top14 Abundant Protein Depletion Midi Spin Columns” from Thermo Scientific. This will remove proteins like albumin and transferrin so that we can produce an optimal image to visualize our proteins.

Keywords : O-GlcNAc; placenta; proteins; western-blot

Shayma Ouala – Lille University; France.
Dawn Wenzel, PhD
MCW Department of Biochemistry

DISCOVERING NEW SMALL MOLECULE BINDERS TO ULK3 KINASE.

Background

ULK3 is a protein kinase that regulates the timing of cytokinetic membrane abscission. ULK3 delays abscission through inhibition of the membrane protein complex called Endosomal Sorting Complexes Required for Transport (ESCRT) proteins. In addition to regulating cytokinesis, ULK3 also functions in hedgehog signaling and autophagy, and its overexpression is linked with increased cell proliferation in several cancers. Therefore, designing a specific ULK3 inhibitor would permit new therapeutic treatments to cancer, and be a tool for understanding ULK3 biology. However, we currently lack small molecules that specifically regulate ULK3 activity. A recent study by Offensperger et al., 2024, discovered four small molecule called fragments that bound to ULK3 using high throughput screening approaches in cells. Chemical fragment ligands can serve as good starting points for the design of specific inhibitors.

In Wenzel lab, the objective is to validate whether these fragments bind directly to ULK3 or not.

Method

In E.coli bacteria, ULK3 kinase was expressed as a HIS-tag protein and purified through Nickel chromatography, anion exchange and gel filtration. Of the four fragments reported by Offensperger et al., one of the fragments (Fragment 1) was commercially available, and two fragments (Fragment 2 and Fragment 3) were purchased as carboxyl precursors that were modified to the amine form by Rob Keyes in the Program of Chemical Biology at MCW. The fourth fragment could not be sourced commercially. Once purified; the binding of the three fragments was studied using the Nano-DSF technique (Nano-differential scanning fluorimetry) which can detect changes in protein stability when a small molecule is bound.

Results

After each step, SDS-PAGE gels were used to check on the progress of the protein expression and its purification. On the three different fragments, we have found that the fragment 3 actually binds to ULK3, as indicated by a $\sim 5^{\circ}\text{C}$ difference between the ΔT_{ms} of the ULK3 kinase domain alone and the ULK3 kinase domain plus Fragment 3. No binding was detected with Fragments 1 and 2.

Conclusion

The Protein ULK3 kinase has been studied and a binding on a fragment has been discovered. This will allow us to continue the research by using the MicroScale Thermophoresis (MST) to measure the affinity of the interaction between the fragment and the kinase.

Title: Decoding Sex-Specific Chronic Stress Effects on the Prelimbic Prefrontal Cortex: The Influence of REDD1/mTORC1 Signaling

Authors: A. Ramanujam^{1,2}, V. Guda², M. K. Estes², B. Kurtoglu², D. Rodrigues de Oliveira², J. R. Mantsch²

Affiliations:

1- College of Arts and Sciences, Loyola University Chicago

2- Department of Pharmacology and Toxicology, Medical College of Wisconsin

Chronic stress triggers molecular changes in the brain, particularly the overexpression of DDIT4 (DNA damage-inducible transcript-4 protein also known as REDD1/Dig2/RTP801), an inhibitor of mTOR (mammalian target of rapamycin complex-1). Glucocorticoids increase the levels of REDD1, leading to reduced dendritic spine growth and impaired synaptic plasticity, which are associated with stress-related disorders like major depressive disorder (MDD) and post-traumatic stress disorder (PTSD). Previous studies in our lab have revealed that REDD1 overexpression in the pre-limbic cortex (PrL), chronic unpredictable stress (CUS) and chronic corticosterone (CORT) elevation-induced deficits in approach motivation behavior for males but not females. However, the molecular mechanisms underlying these changes have not yet been fully investigated. Our study investigates the effects of CUS or chronic oral CORT exposure on the REDD1/mTOR pathway in the pre-limbic cortex. We are looking for a therapeutic target in the pathway. Additionally, we are analyzing sex differences in REDD1/mTOR signaling in rats. We utilized CUS or chronic oral CORT water exposure paradigms to study the effects on REDD1 protein expression in mTORC1 signaling via Rheb in the PrL cortex, an area associated with emotional regulation and decision making. Adult male and female Sprague-Dawley rats (3-4 months old) were randomized and allocated into 2 groups per paradigm (control and experimental): CUS (twice daily stress exposure over 14 days) or oral exposure to 50 µg/mL of CORT over 14 days in the drinking water. After their respective paradigm, animals were decapitated 4 hours after the last stressor. PrL was then micro dissected and fresh-frozen in liquid nitrogen for synaptosome extraction and subsequent western blot analysis. We found that both CUS and chronic oral CORT exposure increased REDD1 protein expression and decreased phospho-p70 ribosomal S6 kinase (S6K), phospho-AKT (Thr 308) and phospho-raptor in males. Ongoing studies are examining effects in female rats. Our findings support the hypothesis that chronic stress alters the expression of proteins involved in REDD1/mTOR pathway. The data provides insights into potential molecular targets for interventions in stress-related disorders such as MDD and PTSD. Further research is warranted to explore the role of REDD1/mTORC via Rheb signaling in modulating stress-induced neuroplasticity and to develop targeted treatments for stress-related psychiatric conditions.

Key-words: REDD1, mTOR, Chronic stress, sex difference, PrL

2,5-Dimethoxy-4-iodoamphetamine (DOI) regulates spine density and immediate early gene expression in the striatum

Peter Tagalakis¹, Jayashree Natajaran², Rutuja Borawke², John McCorvy³, Coti Garcia Keller², Jennifer Tuscher²

1. University of Wisconsin-Parkside

2. MCW Department of Pharmacology and Toxicology

3. MCW Department of Cell Biology, Neurobiology, and Anatomy

Serotonergic psychedelics, including 2,5-Dimethoxy-4-iodoamphetamine (DOI), have garnered significant interest for their potential therapeutic benefit in treating substance use disorders, post-traumatic stress disorder, and depression^{1,3,5,6,8}. DOI is one of several psychedelics that serves as an agonist for the 5-hydroxytryptamine receptor 2A (5HTR_{2A}). Although several recent studies have focused on psychedelic effects in the prefrontal cortex^{2,4,7}, less is known regarding the effects of psychedelics in striatal regions like the Nucleus Accumbens (NAc), which also expresses serotonin receptors, including 5HTR_{2A}. Due to its association with motivation and positive and negative reinforcement, it is an excellent target for the treatment of depression and substance abuse. To test the hypothesis that DOI can similarly regulate spine density and plasticity-related gene expression in the striatum, we used a combination of *in vivo* and *in vitro* approaches. First, we administered 2 mg/kg DOI or saline vehicle to male and female rats intraperitoneally and monitored behavioral responses for 30 minutes. We found that 2mg/kg DOI significantly increased wet dog shake responses in female rats, a behavioral readout of serotonergic system activation in rodents hypothesized to parallel some of the perceptual changes experienced by humans on psychedelic compounds. Rats were transcardially perfused 24 hours later, and tissues were sectioned for spine density analysis. We found DOI also increased spine density in the NAc of female but not male rats. To examine whether DOI also influences plasticity-associated gene expression. We treated striatal neuronal cultures with varying doses of DOI and measured activity-dependent gene expression across several time points thereafter. RT-qPCR analysis of immediate early genes (IEGs) revealed a significant increase in *Fos*, *Arc*, and *Fosb* in striatal neurons 2 hours following DOI treatment. These effects steadily decreased yet were still present 24 hours later. To ask if the observed changes in gene expression were regulated via 5HTR_{2A}, cultures were pre-incubated with the selective 5HTR_{2A} antagonist MDL-100,907 for 30 minutes before DOI treatment. Pre-treatment with MDL substantially blunted DOI induction of IEGs, suggesting their expression is regulated in part by 5HTR_{2A}. Ongoing experiments will continue to explore the role of 5HTR_{2A} in mediating DOI's effects in the striatum by using a CRISPR interference strategy to knock down *Htr2a* selectively. Ultimately, this approach will improve our understanding of the mechanisms through which DOI regulates neuroplasticity in the NAc and aid in developing better therapeutic strategies for treating depression or substance use disorders.

References

1. Canal, C. E., & Morgan, D. (2012). Head-twitch response in rodents induced by the hallucinogen 2,5-dimethoxy-4-iodoamphetamine: a comprehensive history, a re-evaluation of mechanisms, and its utility as a model. *Drug testing and analysis*, 4(7-8), 556–576. <https://doi.org/10.1002/dta.1333>
2. Desouza, L. A., Benekareddy, M., Fanibunda, S. E., Mohammad, F., Janakiraman, B., Ghai, U., Gur, T., Blendy, J. A., & Vaidya, V. A. (2021). The Hallucinogenic Serotonin2A Receptor Agonist, 2,5-Dimethoxy-4-Iodoamphetamine, Promotes cAMP Response Element Binding Protein-Dependent Gene Expression of Specific Plasticity-Associated Genes in the Rodent Neocortex. *Frontiers in Molecular Neuroscience*, 14, 790213. <https://doi.org/10.3389/fnmol.2021.790213>
3. Griffiths, R. R., Johnson, M. W., Carducci, M. A., Umbricht, A., Richards, W. A., Richards, B. D., Cosimano, M. P., & Klinedinst, M. A. (2016). Psilocybin produces substantial and sustained decreases in depression and anxiety in patients with life-threatening cancer: A randomized double-blind trial. *Journal of psychopharmacology (Oxford, England)*, 30(12), 1181–1197. <https://doi.org/10.1177/0269881116675513>
4. Ly, C., Greb, A. C., Cameron, L. P., Wong, J. M., Barragan, E. V., Wilson, P. C., Burbach, K. F., Soltanzadeh Zarandi, S., Sood, A., Paddy, M. R., Duim, W. C., Dennis, M. Y., McAllister, A. K., Ori-McKenney, K. M., Gray, J. A., & Olson, D. E. (2018). Psychedelics Promote Structural and Functional Neural Plasticity. *Cell reports*, 23(11), 3170–3182. <https://doi.org/10.1016/j.celrep.2018.05.022>
5. Mithoefer, M. C., Wagner, M. T., Mithoefer, A. T., Jerome, L., Martin, S. F., Yazar-Klosinski, B., Michel, Y., Brewerton, T. D., & Doblin, R. (2013). Durability of improvement in post-traumatic stress disorder symptoms and absence of harmful effects or drug dependency after 3,4-methylenedioxymethamphetamine-assisted psychotherapy: a prospective long-term follow-up study. *Journal of psychopharmacology (Oxford, England)*, 27(1), 28–39. <https://doi.org/10.1177/0269881112456611>
6. Noller, G. E., Frampton, C. M., & Yazar-Klosinski, B. (2018). Ibogaine treatment outcomes for opioid dependence from a twelve-month follow-up observational study. *The American journal of drug and alcohol abuse*, 44(1), 37–46. <https://doi.org/10.1080/00952990.2017.1310218>
7. Shao, L. X., Liao, C., Gregg, I., Davoudian, P. A., Savalia, N. K., Delagarza, K., & Kwan, A. C. (2021). Psilocybin induces rapid and persistent growth of dendritic spines in frontal cortex in vivo. *Neuron*, 109(16), 2535–2544.e4. <https://doi.org/10.1016/j.neuron.2021.06.008>
8. Zarate, C. A., Jr, Singh, J. B., Carlson, P. J., Brutsche, N. E., Ameli, R., Luckenbaugh, D. A., Charney, D. S., & Manji, H. K. (2006). A randomized trial of an N-methyl-D-aspartate antagonist in treatment-resistant major depression. *Archives of general psychiatry*, 63(8), 856–864. <https://doi.org/10.1001/archpsyc.63.8.856>

Riya Tanwar – University of Wisconsin-Madison

Gareth Pollin, PhD

Linda T. and John A. Mellows Center for Genomic Sciences and Precision Medicine

Targeting PRMT5 Pathways to Disrupt Stress Granule Survival Mechanisms in Pancreatic Cancer

Background

Pancreatic cancer has a 5-year relative survival rate of less than 13%. The most common and aggressive form of pancreatic cancer is Pancreatic Ductal Adenocarcinoma (PDAC), in PDAC high expression of Protein Arginine Methyltransferase 5 (PRMT5) is associated with a worse prognosis and decreased overall survival. During oncogenic stress PDAC cells can form membrane-less organelles consisting of mRNA and proteins called stress granules, which enhances chemotherapy resistance. Cells form stress-granules in response to cellular stress preventing the cell from performing translation to save its genetic information until the stress is alleviated. Stressors can include infections, toxicity, and cancer. While stress granule formation is meant to stop apoptosis and allow the cell to recover, in cancer this mechanism protects the damaged cell from chemotherapy and may reduce its efficacy.

We hypothesize that PRMT5 regulates stress granule assembly through methylation and substrate adaptor binding activity in MiaPaca-2 Cells. Therefore, inhibition of PRMT5 will dysregulate the assembly and dynamics of stress granules formation while under stress caused by an arsenite treatment.

Methods

Cells from a human pancreatic cancer cell line, MIA PaCa-2, were grown in an incubator at 37 degrees Celsius and in 5% CO₂. DMEM media was used with 10% FBS and antibiotics (Penicillin and Streptomycin). The inhibitors used were EPZ015938 (EPZ), which binds to the catalytic site of PRMT5 to inhibit methylation, and BRD0639 (BRD) which binds to the substrate adaptor site and disrupts the interaction between PRMT5 and pICln, RIOK1, and COPR5. The cells were treated with two doses of EPZ or BRD at an interval of 12 hours, and then 100 uM of arsenite for one hour.

Immunofluorescence was then used to visualize stress granules. The images of the cells from the immunofluorescence were analyzed using Image J and data such as the number of stress granules, the size of the stress granules, and the number of cells in the image were recorded.

Results

We observed that EPZ (P-value = 0.000187) and BRD (P-value = 0.001383) had significantly less stress granules per cell in comparison to the DMSO control when under arsenite stress. Further investigations found a dysregulation in methylation, EPZ (P-value = 0.001982) had a significantly less overlap with SDMA than DMSO under arsenite stress and BRD (P-value = 0.100238896) showed no significant difference.

Conclusion

PRMT5 regulates stress granule assembly through both methylation and substrate adaptor binding activity in MIA PaCa-2 Cells. When PRMT5 binding was inhibited, the assembly and size of stress granules were lessened, and different proteins were methylated depending on the treatment. This holds relevance for the biochemical impact of stress-granule related chemotherapy resistance and highlights the importance of further research in to targeting PRMT5 in PDAC.

Heterotypic dual-vector ITRs increase efficiency in animal transgenesis

Background

Adeno-associated virus (AAV) is used to produce transgenic animal models to study human physiology. AAV's transduction of large transgenes is limited by its relatively small 4.7 kb capacity, but it has been shown to be overcome by a method utilizing a homotypic ITR dual-vector system, although with low efficiency. However, by utilizing a heterotypic ITR system compared to a homotypic ITR system, the low efficiency can be overcome and suggests a method of increasing transgenesis of large transgenes by utilizing a heterotypic ITR dual-vector AAV.

Method

rAAV plasmids AV5:2donor, AV2:5acceptor, and AVrep5 plasmids were received from Dr. Ziyang Yan's lab at the University of Iowa. Primers were made for these three vectors and were sent for DNA sequencing. These vectors were used to transform DH5 α competent bacteria cells and plated on ampicillin-containing LB plates. Four isolated colonies were chosen per plasmid vector for screening using a miniprep to purify their plasmids. Purified plasmids were restriction digested using ApaI and confirmed on gel electrophoresis. Correctly transformed plasmids were grown in glycerol stocks. Further steps include sending the purified plasmids to Dr. Daniel Lipinski's lab in the MCW eye institute and transforming them into AAV-1 virus. As proof of concept, HeLa cells would be grown and transduced with either the heterotypic or homotypic viral vectors, each containing half of the LacZ gene. X-gal staining would be utilized to observe the rate at which the AAV transduced the cells and the rate of recombination between the dual vectors.

Results

Bacterial growth on the LB-amp media confirmed transformation using our three plasmids. The miniprep resulted in absorbance ratios of A260:280 and A260:230 as ~1.8 and ~2.2, respectively, indicating pure isolated plasmid. The restriction enzyme showed predicted bands for all 12 lanes indicating that all of the transformed bacteria had the correct plasmid insertion. The transduced HeLa cells with the heterotypic ITR vectors would be expected to show a greater percentage of blue HeLa cells compared to the heterotypic ITR vectors.

Conclusion

From the presence of greater blue staining from the HeLa cells transduced with the heterotypic ITR vectors compared to the homotypic ITR vectors, this data would suggest that heterotypic

ITR vectors have greater efficiency at transducing HeLa cells. This could then be further applied to embryos, suggesting that transduction of larger transgenes can be done at a greater rate by utilizing a heterotypic ITR dual vector system with AAV.

Bao Ngoc Dinh – Kenyon College
Daisy Sahoo, PhD,
MCW Department of Biochemistry

The Role of Modified HDL in Pro-atherogenic Signaling Cascades

Atherosclerosis, a major cause of cardiovascular disease, is a progressive disease that involves the buildup of fats, cholesterol and other substances on the artery walls (plaque). Plaques can cause arteries to narrow, blocking blood flow and increasing the likelihood of heart attack. High-density lipoproteins (HDL) play important roles in the pathogenesis of atherosclerosis due to its cardioprotective roles in removing peripheral cholesterol, along with its anti-inflammatory and antioxidant properties. Recent studies from our lab have demonstrated that HDL modified by reactive aldehydes has impaired cardioprotective properties in macrophages such as decreased macrophage migration, along with impaired ability to facilitate key steps in reverse cholesterol transport. Our goal in this study is to test the hypothesis that modification of HDL results in decreased macrophage migration. Specifically, we wanted to investigate the phosphorylation status of the MAP kinase pathways (ERK, JNK, p38) in macrophages treated with native HDL and modified HDL as these pathways are involved in macrophage migration. In order to do this, we modified HDL with malondialdehyde (MDA), and verified successful modification via immunoblot analyses. Next, we isolated peritoneal macrophages from wild-type (WT) and CD36 KO mice to compare the levels of phosphorylation of various signaling proteins of the MAP kinase pathways in the presence of native vs MDA-HDL. To do this, WT and CD36 KO mice were injected with thioglycolate and macrophages were harvested from peritoneal cavity, plated and incubated at 37°C for 24 hours. After that, macrophages were treated with native and MDA-HDL, and cells were lysed to collect cellular lysates. Preliminary data suggest that MDA-HDL delayed ERK 1/2 activation in WT macrophages while native HDL stimulates JNK in WT macrophages. Taken together, the data suggest that MDA-HDL may have a delayed activation period in comparison to native HDL in macrophages.

Key words: Cardiovascular disease, atherosclerosis, modified high-density lipoprotein (HDL), malondialdehyde (MDA), MAP kinase pathways

Resistin Increases Cholesterol in Macrophages Contributing to Atherosclerosis

Background

Cardiovascular disease (CVD) remains the leading cause of death worldwide. Atherosclerosis, a condition characterized by the development of arterial plaques, is a primary contributor to heart attacks and strokes and serves as a key indicator of CVD progression. The pathogenesis of atherosclerosis involves various inflammatory pathways, with macrophages playing a crucial role in plaque formation. Macrophages are specialized immune cells that typically function to eliminate dead cells, debris, and metabolize substances like low-density lipoprotein (LDL) – a form of cholesterol. These cells possess specific receptors that enable the recognition and uptake of cholesterol. One such receptor, cluster of differentiation 36 (CD36), recognizes oxidized LDL (oxLDL), a modified form of cholesterol resulting from the interaction between LDL and reactive oxygen species. While macrophages normally process oxLDL as part of cholesterol metabolism, excessive uptake can lead to their transformation into foam cells - swollen, dysfunctional cells that are a primary component of atherosclerotic plaques. This paper will examine the effects of resistin, a protein that appears to upregulate CD36 production, thereby potentially increasing foam cell formation and contributing to the progression of atherosclerosis.

Method

This experiment used mouse macrophages - Wild type (WT) and CD36 knock-out (CD36 KO). Macrophages were extracted and treated with 4.0 nmol/L resistin (48 hours) and 20 µg/mL oxLDL (24 hours). Cells were incubated with 1640 RPMI medium with fetal bovine serum. The cells were analyzed via flow cytometry and cholesterol assay to detect CD36 presence and cholesterol concentration, respectively.

Results

The results of the cholesterol assays indicated a significant increase in cholesterol uptake in WT macrophages treated with resistin and oxLDL compared to control WT macrophages. When comparing WT and CD36 KO cells, greater cholesterol uptake was observed in all CD36 KO groups, except those treated with resistin and oxLDL. Although the differences were not statistically significant, these findings may suggest a potential role for resistin in modulating cholesterol levels in macrophages. Additionally, the flow cytometry results did not reveal a statistically significant increase in CD36 production among any of the treated macrophage groups compared to the control cells. This lack of effect suggests that resistin does not influence CD36 production, indicating that resistin may contribute to atherogenesis through a different mechanism.

Conclusion

Resistin appears to play a significant role in atherogenesis, as indicated by the cholesterol uptake data; however, it does not seem to regulate CD36. The precise mechanism by which resistin enhances cholesterol uptake requires further investigation, and additional trials are necessary to strengthen the conclusions drawn from this study. Atherosclerosis is a complex condition to treat, but continued research in this area could have a profound impact on global human health.

Audrey Catlin – University of Wisconsin-Madison
Karina Bursch and Brian Smith, PhD
MCW Department of Biochemistry

PBRM1-BD2 and PBRM1-BD4 missense variants associated with clear cell renal cell carcinoma impact protein structure and ligand binding

The tumor suppressor protein Polybromo-1 (PBRM1) is a subunit of the chromatin-remodeling Polybromo, Brahma-related gene 1 (BRG1)-associated factors (PBAF) complex. PBRM1 contains six bromodomains, which are epigenetic ‘reader’ modules responsible for PBRM1 binding to acetylated lysine residues on histone tails and other nuclear proteins. PBRM1 is the second most mutated protein in patients with clear cell renal cell carcinoma (ccRCC), the most common type of kidney cancer. ccRCC patients with PBRM1 mutations that inhibit protein expression have a greater survival rate and respond better to many cancer therapies, such as immunotherapy. However, many patients possess PBRM1 missense mutations that cluster in PBRM1 bromodomains and may result in full-length protein expression. These PBRM1 missense variants are largely uncharacterized. To identify the impact of PBRM1 bromodomain missense variants on cancer patients’ treatment success, the structure and binding of these variants must be compared to the wild-type (WT) protein. We performed *in vitro* biophysical analysis for PBRM1-bromodomain 2 (BD2) and PBRM1-bromodomain 4 (BD4) WT and select missense variants with nano differential scanning fluorimetry (nanoDSF) to quantify protein thermal stability. We also used AlphaScreen assays and electrophoretic mobility shift assays to measure protein binding to acetylated histone tail peptides and DNA. We show that PBRM1-BD2 and PBRM1-BD4 missense variants displayed variant-specific effects on protein structure and ability to bind to acetylated histone and DNA ligands in a manner dependent on location of the affected residue in the bromodomain and residue conservation. The knowledge gained from these *in vitro* biophysical assays will impact future analysis of PBRM1 missense variants found in cancer patients and create a pathway to stronger application of precision medicine in the clinic.

MICHAELA HAENSGEN – MILWAUKEE SCHOOL OF ENGINEERING
VERA TARAKANOVA PhD,
MCW DEPARTMENT OF MICROBIOLOGY AND IMMUNOLOGY

**EFFECTS OF GAMMAHERPESVIRUS INFECTION ON LIPOPROTEIN TRANSPORTER
SR-BI**

Background

Gammaherpesviruses are double-stranded DNA viruses that affect over 95% of adults worldwide. The known human virus strains are Epstein-Barr virus (EBV) and Kaposi's sarcoma-associated herpesvirus (KSHV), both of which are linked to various types of cancers, such as lymphomas. Studying these viruses is challenging because EBV and KSHV only infect humans, it is difficult to determine the timing of infection, and most adult human cells have experienced previous infection. Consequently, murine herpesvirus (MHV-68) has been used to study the initial viral exposure in mice. MHV-68 is similar to EBV and KSHV, allowing researchers to infect naïve mice in a controlled manner and study first infection. This model also provides the opportunity to manipulate mouse genetics and further investigate the impact of viral infection. Previous research has shown that cholesterol and fatty acid synthesis support gammaherpesvirus replication. It is understood that lipid synthesis pathways facilitate the lytic replication of the virus, as characterized in cell lines or primary cells. However, less is known about lipid synthesis and transport in vivo. Our aim is to further characterize viral infection through changes in mRNA and protein levels of the primary high-density lipoprotein (HDL) receptor, scavenger receptor class B type 1 (SR-B1).

Method

We utilized bone marrow-derived macrophages (BMDM) from mice, as the virus establishes latency in this cell type and macrophages play a significant role in cholesterol metabolism and homeostasis. The cells were infected with MHV-68 in media or mock infected with media and then collected 24 and 48 hours after infection. The mRNA levels were measured by qPCR and analyzed using delta-delta Ct method. The protein levels were measured by Western Blotting and analyzed using densitometry.

Results

The levels of mRNA expression of Scarb1, the gene involved in making SR-BI, was measured along with Gapdh to determine the relative fold gene expression. There was no significant change in Scarb1 levels at 24 and 48 hours post mock or MHV-68 infection. We faced challenges in quantifying SR-B1 protein levels, likely due to blocking or antibody issues.

Conclusion

Our findings indicated that SR-B1 mRNA levels are unaffected by MHV-68 24 and 48 hours post infection; however, more time points should be studied with a focus on early infection. As for the effect of infection on SR-B1 protein levels, this remains unclear. Future work will involve the continued optimization of the Western Blotting procedure to thoroughly quantify the effects of MHV-68 infection on SR-BI.

Investigating MltG Regulation in *Enterococcus faecalis* Antibiotic Resistance

Background

Enterococci are opportunistic pathogens present within the human gut as commensal microbes. Their resistance to antibiotics allows them to grow when antibiotic treatments, for other illnesses, eliminate other microbes. This can result in lethal difficulties since their antibiotic resistance prevents most cell-wall antibiotic treatment from being effective. Enterococci can acquire resistance to vancomycin, an antibiotic that interferes with bacterial cell wall synthesis resulting in cell wall stress. This resistance to vancomycin is significantly reduced by deletion of MltG, a cell wall hydrolase predicted to be involved in peptidoglycan synthesis. The importance of MltG expression for vancomycin resistance prompted investigation into the regulation of MltG expression. Other enterococcal genes that aid responses to cell wall stress are known to be regulated by a two-component system, CroRS. CroS recognizes cell-wall stress and phosphorylates CroR which, in turn, activates gene expression to support stress resistance. RNAseq previously performed within the lab found that MltG was slightly upregulated in a CroR dependent manner. The Kristich lab discovered that CroR has a specific motif upstream of its regulon genes to promote their expression; this motif is found upstream of MltG. We hypothesize that MltG is upregulated in response to stress in a CroR dependent manner.

Method

To test if MltG is upregulated in response to stress or in a CroR dependent manner, wildtype or *ΔcroR* cells were grown to an exponential phase and then treated with or without vancomycin (to stimulate stress) to use in the following assays. We then utilized western blots to analyze MltG protein levels and qRT-PCR to analyze MltG transcript levels. We also utilized a reporter assay to analyze MltG promoter activity. We constructed a MltG promoter-*lacZ* fusion and expressed it in the strains and conditions previously described.

Results

The western blots and the qRT-PCR indicated that the MltG expression is regulated in a CroR independent manner; however, the expression in response to stress was less conclusive. The Beta-galactosidase reporter assay confirms that the promoter of MltG drives similar levels of expression regardless of stress or CroR presence.

Conclusion

MltG does not seem to be upregulated in a CroR dependent manner; however, there are some indications it may be upregulated in response to stress. Therefore, further experimentation is recommended. However, we can reject our initial hypothesis that MltG is upregulated in a CroR dependent manner.

Neva Bergemann – Carthage College

Bonnie Dittel, PhD

Versiti Blood Research Institute and Department of Microbiology and Immunology, Medical College of Wisconsin

Investigating the Impact of CCR7 expression in B cells on T Regulatory Cell Proliferation

Background

Multiple sclerosis (MS) is the most common autoimmune disease of the central nervous system (CNS) which is characterized by immune-mediated demyelination of the brain and spinal cord nerves. FoxP3⁺CD4⁺ regulatory T cells (Tregs) play a vital role in suppressing the immune response and reducing autoimmunity. Our lab has previously identified the B cell subset B cell IgD Low (BD_L) that expresses glucocorticoid-induced tumor necrosis factor receptor ligand (GITRL) which interacts with its receptor (GITR) on Tregs, promoting Treg proliferation. Mice lacking B cells (JH^{-/-}) have reduced numbers of Treg and cannot recover from experimental autoimmune encephalomyelitis (EAE), the mouse model of MS. The adoptive transfer of BD_L into JH^{-/-} lead to an increase in Treg in a GITRL-dependent BD_L manner and recovery from EAE. Both Tregs and BD_L express a chemokine receptor called CCR7, which guides their movement to areas in secondary lymphoid organs, like the spleen, where they can interact. By altering CCR7 levels, we can potentially enhance the colocalization of BD_L and Tregs, thereby boosting Treg proliferation through increased GITR engagement. While investigating other B cell lines that share surface marker expression to BD_L the mouse B-cell lymphoma WEHI-231 cell line was found to simulate BD_L through the expression of CCR7 and GITRL. When the functionality of WEHI-231 cells were compared to BD_L in JH^{-/-} mice, the WEHI-231 cells displayed higher Treg proliferation, reaching levels similar to those in wild-type mice. Therefore, WEHI-231 cells can serve as a model cell line to study the importance of CCR7 expression in B cells for Treg proliferation. We hypothesize that adoptively transferring WEHI-231 cells sorted to express high GITRL (GITRL^{HI}) will increase Treg proliferation, whereas WEHI-231 cells sorted to express low CCR7 (CCR7^{LO}) will decrease Treg proliferation when compared to unsorted WEHI-231 cells in JH^{-/-} mice.

Method

Fluorescence-activated cell sorting (FACS) was used to purify both GITRL^{HI} and CCR7^{LO} cell groups for subsequent culturing. GITRL^{HI} and CCR7^{LO} expression in sorted WEHI-231 cells was analyzed through flow cytometry after seven days of culture and before adoptive transfer into JH^{-/-} mice.

Results

Due to unforeseen challenges with cell culture and sorting of the WEHI-231 cells, no data regarding Treg proliferation is yet available. However, preliminary results found that WEHI-231 CCR7^{LO} cells remain stable and maintain their low expression levels after a week of continuous culture, whereas WEHI-231 GITRL^{HI} did not.

Conclusion

Future work aims to quantify the results of the adoptive transfer of WEHI-231 and CCR7^{LO} B cells through flow cytometry analysis of the processed spleens of JH^{-/-} mice. We expect to observe decreased Treg proliferation in JH^{-/-} mice that receive our WEHI-231 CCR7^{LO} cells than compared to unsorted WEHI-231 cells. This work will validate if CCR7 is essential for B cell and Treg colocalization and Treg proliferation.

Felicity Giampietro – The Catholic University of America, MCW SPUR Program
Casey Zoss, BS Medical College of Wisconsin, MSTP Program
Christopher Chitambar, MD
Kathleen Schmainda, PhD
MCW Department of Biophysics

Identification of factors influencing sensitivity of glioblastoma cells to gallium maltolate

Background:

Glioblastoma (GBM) is the most aggressive primary brain tumor with a median survival of 20.9 months following current treatment, with limited treatment options following relapse. Increased iron uptake and metabolism drive rapid proliferation of GBM cells, making iron-targeting treatments a promising therapeutic strategy. Gallium is a metal that interferes with cellular iron (Fe) uptake and metabolism. Gallium maltolate (GaM) is an orally bioavailable gallium drug found to inhibit growth of GBM cells *in vitro* and to dramatically extend survival *in vivo*. A phase I clinical trial of GaM for relapsed GBM is underway at MCW. To maximize the likelihood of success, identifying biomarkers of resistance to GaM is crucial. Past studies showed CCRF-CEM (lymphoma) cells pre-exposed to zinc displayed decreased sensitivity to gallium nitrate, a first-generation gallium drug. Similarly, HL60 (leukemia) cells co-incubated with iron were found to have decreased sensitivity to gallium nitrate. Here, we investigate if the same factors affecting CCRF-CEM and HL60 cell sensitivity to gallium nitrate translate to GBM cells treated with GaM.

Methods:

The D54 human glioblastoma cell line was pre-incubated with 50 μM zinc sulfate for 72hr before GaM treatment (10-100 μM). MTT cell proliferation assays were performed every 24hrs for 96hrs. In a separate experiment, D54 cells were co-incubated with 50 μM or 100 μM iron salt (ferric ammonium citrate [FAC]) and GaM treatment (10–100 μM). Using an Incucyte incubator/imager, proliferation was calculated every 4hr for 96hr.

Results:

MTT assays reveal no difference in cell viability between D54 cells pre-incubated with Zn versus control cells at any timepoint. The groups also have similar IC50s. Unlike CCRF-CEM cells, 50 μM zinc sulfate pre-incubation appears not to affect D54 sensitivity to GaM. Incucyte data show that GaM inhibits cell growth at early timepoints and kills cells at later timepoints. Co-incubation with the highest concentration of FAC (100 μM) displayed greater proliferation than co-incubation with the lower concentration FAC (50 μM) or GaM alone. The data indicate that iron levels are indeed a factor affecting GBM cell sensitivity to GaM and suggest competition between gallium and iron in tumor growth.

Conclusions:

Understanding the role of iron-dependent processes that influence GBM sensitivity to GaM has implications for identification of patients for whom GaM would be of greatest benefit. This finding also presents new avenues for investigating synergy between GaM and tumor iron-depleting drugs, such as iron chelators.

Keywords: Glioblastoma, gallium maltolate, iron

Abbreviations: IC50 = drug concentration that inhibits cell growth by 50%

Leveraging Generative Adversarial Networks for Generating Non-Invasive Prostate Cancer Histopathology

Background:

Prostate cancer is the most diagnosed cancer in men, with an estimated 34,700 deaths expected in the USA this year. The current diagnostic process for prostate cancer begins with detecting elevated PSA levels, followed by magnetic resonance imaging (MRI) and biopsy. If cancer is found at biopsy, surgical excision of the prostate may be performed. This procedure produces whole mount histology slides that are pathologically assessed to determine the Gleason score, which indicates the aggressiveness of the cancer. However, this method requires the removal of prostate tissue before determining the Gleason score and involves an invasive procedure that may lead to infections. This study investigates the potential of using Generative Adversarial Networks (GANs) to convert MRI data into synthetic histopathology images that closely resemble actual histopathological samples. The hypothesis is that GANs can generate accurate histopathological images from MRI data, enabling the determination of the Gleason level pre-biopsy and facilitating the construction of larger histopathological datasets. To test this hypothesis, the aim is to evaluate the feasibility and accuracy of GAN-generated histopathology images compared to the original Gleason scores.

Method:

The dataset consisted of 249 3D MRI and corresponding histology images, with each 3D image containing 20-44 slides. However, only three slides per histology image were significant for analysis. As the rest of the 3D histology image slides are blank. After preprocessing, 685 paired masked MRI and histology images were usable for the experiment. We utilized a pix2pix GAN model for MRI-to-histology translation, employing a U-Net generator designed for 512x512 images and a PatchGAN discriminator. Additionally, a fine-tuned ESRGAN model was used to enhance the resolution of the histology images, allowing closer analysis by another model or radiologist. Training involved monitoring loss for both the generator and discriminator, with success determined by visual inspection of the output images.

Results:

The pix2pix model generated grayscale images closely resembling histology slices, outperforming models such as GcGAN. Further training on a smaller, colored co-registered histology dataset yielded stained synthetic histology images. The ESRGAN model achieved results up to eight times the MRI's resolution, compared to Real-RESGAN, super-resolution CNNs, super-resolution autoencoders, and bicubic interpolation. However, ESRGAN was trained on 512x512 patches, while the synthetic histology images contained prostates only within 100-200 pixels squared.

Conclusion:

This research demonstrated the effectiveness of various GAN models in generating synthetic histopathology images from MRI data. The pix2pix model successfully generated stained histology images, while ESRGAN produced high-resolution images closer to whole-mount histology images. This study highlights the potential of advanced computational models like GANs in medical imaging. Future research will focus on enhancing resolution without losing critical features, increasing the clinical applicability of generated images, and potentially integrating Brownian Bridge Diffusion within the U-Net generator for improved image-to-image translation.

Keyword's – MRI, Prostate Cancer, GAN, Super Resolution, Image-to-Image translation, U-net, Histology

Enhancing Large Language Models with Preference Expression: Weight Modification of the Gemma LLM for Improved AI Interaction and Bias Mitigation

Background

In the evolving field of artificial intelligence, enhancing the behavioral characteristics of large language models (LLMs) is critical for improving their human-like interaction. This study aimed to modify the weights of the Gemma LLM to develop and exhibit preferences. This enhancement is expected to lead to more nuanced and opinionated responses, thus advancing the model's applicability in various AI-driven tasks. While having more human-like interactions is nice in many cases, human-like interactions can bring non-ideal human-like behaviors, including bias, into outputs. Notably, in the medical field, modifications to remove preferences can help ensure that AI systems generate unbiased diagnoses and write accurate visit summaries, promoting equitable healthcare outcomes. We hypothesize that targeted weight modifications can provide LLMs with preference-expressing capabilities.

Method

The study utilized a systematic approach to adjust the weight parameters of the Gemma LLM. To achieve this, a series of prompts were designed and administered to probe the ability of the LLM to express preferences. While the Gemma LLM was processing those prompts, the outputs of each neuron in the network were measured to identify portions of the network activated with the prompted tasks. With the activated network identified, its strength and size (both known as 'hyperparameters') were then modulated to change the performance of the LLM. Claude, an AI model from Anthropic, was employed to evaluate Gemma's responses. The evaluation process involved scoring responses on a scale from 0 to 9, where 0 indicated the purpose of the request was fully met, and 9 indicated a complete failure to meet the request. These scores were used to identify optimal hyperparameters for adjusting the weights, focusing on enhancing the model's capability to express preferences.

Results

Modifications to Gemma's weights were found to significantly impact the model's ability to express preferences. The iterative process of adjusting hyperparameters, guided by Claude's scoring, led to a noticeable improvement in the quality and consistency of Gemma's responses. Specific adjustments resulted in an increase in the model's ability to generate preference-indicating responses as per the scoring criteria. Additionally, the enhanced preference expression can help mitigate biases in medical diagnoses and visit summaries, fostering more accurate and fair outcomes.

Conclusion

The results confirm that targeted weight modifications can provide LLMs with preference-expressing capabilities. The study's most significant finding is the enhancement of Gemma's response quality and consistency, showcasing the feasibility of tuning LLMs for specific behavioral traits. This advancement holds promise for developing more interactive and human-like AI models, with important implications for reducing biases in medical applications.

Keywords: large language models, weight modification, preference expression, bias mitigation

Deepa Gayadin – Luther College

Neshatul Haque, PhD; Jessica Wagenknecht; Michael T. Zimmermann, PhD

Linda T. and John A. Mellows Center for Genomic Sciences and Precision
Medicine - Bioinformatics Research and Development Lab

Defining the SMARCA4 Walker regions in 3D and the mechanistic effects of their mutations

Background: SMARCA4 is an ATP-dependent helicase necessary for gene transcription regulation, part of the SWI/SNF chromatin remodeling (BAF) complex. Germline mutations of SMARCA4 are associated with Rhabdoid tumor predisposition syndrome, Coffin-Siris syndrome, ovarian cancer subtypes (e.g. SCCOHT), and are frequently mutated somatically across many human cancer types. This project focused on specific linear motifs essential for helicase function. Namely, the Walker A (GLGKT, 782-786), essential for ATP-Mg⁺² binding, and Walker B (DEGH, 880-883) which facilitates nucleotide hydrolysis. We hypothesized that mutations in the three-dimensional (3D) region around the Walker motifs are also critical for the Walker functions. Therefore, their mutation would be similarly deleterious as directly altering the motif. Importantly, we anticipate that the specific organization of the 3D environment around Walker motifs is also essential for function and will enable us to better understand the requirements of SMARCA4 function, and to mechanistically interpret the genetic mutations observed across human congenital syndromes and somatic diseases.

Methods: To assess the significance of Walker mutations in 3D, we looked at multiple protein structure-based metrics including stability and local flexibility and compared them with genomic pathogenicity predictors. Missense mutations in Walker regions were retrieved from ClinVar, HGMD, COSMOS and GnomAD. Associated scores of metrics looking at functional impact, protein structure and stability were obtained from Ensembl and existing workflows (FoldX and Frustratometer). Final metrics were chosen to reflect a range of methods predicting pathogenicity from a correlation heatmap in R, and finally variants were clustered using these metrics and heatmap generated clustered variants with high consensus on pathogenicity prediction scores.

Results: The pathogenicity predictions from AlphaFold (AM), gMVP, REVEL and VARIETY were high for all the mutations (range: 1 - 0.92), suggesting that they are strongly damaging, aligned with the categorical outcomes such as EVE (all pathogenic) and CADD (>20). The 3D calculations including change in mutation energy, are concordant with the sequence-based pathogenicity score. Furthermore, mutations in Walker regions have known association with rare diseases and cancer. We further carried out detailed structural analysis on wild-type structure to delineate structural and functional role of the walker residues. The data suggest that walker A is mostly involved in stabilizing the N-terminal lobe of the helicase by hydrophobic interaction, however, walker B is observed to stabilize the edge of N-terminal lobe at the interface of N-terminal and C-terminal with a strong interaction network of H-bonding. These structural alterations could potentially contribute to changes of function and hence pathogenic.

Conclusions: The helicase role of the BAF complex is crucial in regulating the general replication and transcription of genetic material. These enzymes have evolved to perform an optimal role in higher organisms. Genetic variation in such regulatory proteins is often very deleterious. Similarly, mutations in the Walker region are mostly associated with cancers and rare diseases. Our study extends knowledge about these key functional sites by defining the Walker region in 3D, because the proper positioning of the motif residues is necessary for their function. Further, our study further provides information on molecular roles of these residues by structural assessment, which suggests that the helicase of SMARCA4 is a dynamically active domain made up of two subdomains. The dynamics in the subdomain and between the subdomains is the key to helicase activity. Further, data suggest that walker A contributes to dynamic stability by hydrophobic interaction and walker B by the network of H-bonding interactions. Thus, our study establishes an important fact about the molecular mechanism of helicase which could be helpful in predicting deleterious role of novel mutations in future.

Morgan Kosch – University of Wisconsin-Madison
Jessica Wagenknecht; Neshatul Haque, PhD; Michael T. Zimmermann, PhD
Linda T. and John A. Mellows Center for Genomic Sciences and Precision
Medicine at the Medical College of Wisconsin

Walker A and Walker B Interpretations of KRAS Protein Genetic Variants

Background:

The KRAS protein activates signal transduction pathways that lead to tumor growth. KRAS is the most frequently mutated RAS family member with mutations found in over 90% of pancreatic tumors, for example. As a GTPase, KRAS cycles between GTP-bound and GDP-bound states, which regulate its ability to bind to other proteins. Specific to its enzymatic function are linear motifs. Two linear motifs are the Walker A and Walker B regions, which contain cancer hotspots due to their necessary role. This study's goal is to characterize hotspot and non-hotspot KRAS Walker mutations regarding nucleotide binding and protein stability. Importantly, we take an expanded view in defining Walker mutations, by investigating the 3D environment around these linear motifs.

Method:

Genomic variants were collected from GnomAD, ClinVAR, and COSMIC. Variant effects were assessed using data from VEP, dbNSFP, FrustratometerR, FoldX, and MAVEdB. Visual analytics were used to assess patterns across scores, which we categorized according to their type. All-versus-all correlation patterns were used to interpret scores and determine their biological equivalence. A final heat map was created to compare the score types with mutations. Six hotspot variants were analyzed in addition to an additional 78 non-hotspot variants present in the Walker three-dimensional regions.

Results

We found the structural measurements of Walker mutations match experimental measurements, and they both are more distinct from pathogenicity prediction scores. Most of the pathogenicity prediction scores predict Walker variants to be pathogenic. For example, 71% of all CADD scores fall above the threshold stated as likely pathogenic. Further, variants of the same location typically have similar scores, however there are exceptions, indicating the need for mutation-specific nuances to be accounted for. We also discovered that, variants near the Mg²⁺ and phosphate binding sites had the greatest impact on ligand binding, while variants further away, including the hotspot variants, had less direct impact on these measures. For example, variants at D57 have a large impact on effector protein binding, specifically SOS1 and DARPinK27. On the other hand, hotspot variants at residues G12 and G13 both have a small impact on structural and effector protein binding yet have a large impact on structural dynamics.

Conclusion

Many of the variant effect prediction scores consider most of the variants pathogenic, therefore it is especially helpful to distinguish variants based on structural and functional scores. Based on the similarities and trends we observe, the location and residue type impact the structural stability and dynamics, especially around the p-loop of Walker A. Effector protein binding was mostly dependent on the location of the variant as well, regardless of if it was known to be a cancer hotspot or non-hotspot. Therefore, studying a multitude of variants was helpful in analyzing the unique impacts each variant had. This finding has importance for precision oncology efforts to tailor approaches to each tumor genomic profile.

Post-Operative Cognitive Dysfunction and its Effects on Attentional Control

Introduction

Cognitive dysfunction following surgery is known to affect as much as 59% of the 60,000 patients undergoing surgical procedures that involve general anesthesia in the United States each day. This project aims to provide data that may ultimately allow us to develop auxiliary therapies that can help limit the effects of cognitive decline associated with general anesthesia. Post-operative cognitive dysfunction (POCD) is defined as an impairment of neural system functioning associated with the administration of general anesthesia during surgery. Most of the published work on POCD and methodology used tends to be too non-specific to accurately identify the cognitive sub-processes (and brain networks) affected. Here, we will borrow sensitive reaction time tasks from the cognitive neuroscience literature to longitudinally measure changes in multiple sub-processes of attentional control pre- to post-operation. Furthermore, sex differences in recovery from anesthesia are well-documented, illustrating the need for additional work focused on the cognitive effects of anesthesia in women. Our study, therefore, targets women being treated for gynecological cancer.

Methodology

The Attention Network Test (ANT) was developed as a stable, sensitive task to quickly assess three key components of selective attention: alerting, orienting, and executive control (i.e., distractor filtering). These sub-processes of attention are well-understood in terms of the network of brain regions subserving them. We have adapted the ANT for use with gynecological cancer patients. To identify the constellation of behavioral and brain-based markers of POCD, we have designed a unique within- and between-subjects, longitudinal experiment in which patients are tested using the ANT at three timepoints: baseline (prior to surgery); 2 weeks post-surgery; and 4 weeks post-surgery. Patients will be categorized as POCD and no-POCD using a validated self-report questionnaire focused on cancer-related cognitive impairment (i.e., FACT-Cog).

Hypotheses

We hypothesize that (a) the cognitive operation of attention is directly affected by POCD, and (b) the sub-process of distractor filtering (and not alerting or orienting) will be selectively affected by POCD. The first hypothesis will be explored by comparing baseline ANT scores to post-op scores separately for the POCD and no-POCD groups. We predict that the no-POCD group will show no change in ANT after surgery, whereas the POCD group will show a significant change. The second hypothesis will be tested by comparing the change in ANT sub-scores pre- to post-op in the POCD group only. We predict that the Distracter Filtering score will show a significant change post-op, but Alerting and Orienting will not. These results may demonstrate that attentional control is affected by general anesthesia and can be a reliable measure of cognitive dysfunction associated with anesthesia. Furthermore, if the distracter filtering sub-process of attentional control is shown to have change after surgery, these results

may demonstrate that neuroinflammation is present in the limited brain regions associated with distractor filtering.

Emily Zhang – Cornell University
Brandon Tefft, PhD
MCW-Marquette Department of Biomedical Engineering

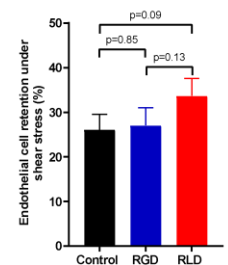
RLD Peptide Enhances Endothelial Retention Under Shear Stress Conditions

Background

Establishing an endothelial monolayer can improve the patency of synthetic grafts (SGs) used in bypass surgeries. When endothelial cells (ECs) are exposed to shear stress induced by physiological blood flow, the loss of a functional endothelium can lead to a cascade of events including thrombogenesis, inflammation, and hyperplasia. Over the past decades, the RGD sequence has been intensively studied for its role in cell adhesion and its potential to help maintain endothelialization. While RGD has been found to promote greater cell retention, the peptide's thrombogenicity limits its clinical application. Therefore, the need remains to find a suitable alternative. In this study, we aim to analyze the RLD (Arg-Leu-Asp) peptide's ability to facilitate endothelial cell retention and compare its efficacy to RGD *in vitro*.

Methods

Human endothelial cells (HAECs) were cultured until 80% confluency. On day 1, pre-treated dishes were coated with 20 μg RGD, RLD, and PBS control respectively. After 24 hours, HAECs were seeded in the flow path region using a rectangular gasket. After cells attached to the surface, fresh media was added to the dish to culture overnight. To assess the retention, shear stress was applied with a parallel plate flow chamber for five minutes. A flow rate of 3.18 mL/min was employed to attain a fluid shear stress of 15 dyn/cm^2 . EC attachment after seeding and retention was assessed by fluorescent microscopy and ImageJ.



Results

Results were obtained from a total of $n=3$ replicates. The preliminary data shows both RGD and RLD enhance cell retention under shear stress, with RLD demonstrating a trend toward greater enhancement, however no statistical significance was achieved between any group. Statistical significance was defined as $p<0.05$.

Conclusion

EC attachment and retention are relatively weak on uncoated prostheses. Preliminary findings from the study indicate that an RLD coating may facilitate greater cell retention upon shear stress *in vitro*, however future work is necessary with larger sample sizes to verify these findings and explore the biological mechanisms behind these observations.

Doriann Pina – Medical College of Wisconsin
Anne Kwitek, Ph.D.
MCW Department of Physiology

**Health Outcomes of PFAS Exposure Through Genetics and Environmental (GxE) Interactions
in Heterogenous Stock Founder Rats.**

Perfluorooctanesulfonate (PFOS) is a type of PFAS known as (per-and poly-fluorinated alkylated substance) which is a manufactured compound chemical made of strong carbon-fluorine bonds and sulfonic acid (ehn.org). Due to its hydrophobic and lipophobic properties, industries use it in food wrappers, fire-fighting foam, sweat-proof clothing, and cosmetics. PFAS is also an Endocrine-Disrupting Chemical (EDC) linked to induced Metabolic syndrome (MetS), which is an association of health disorders including heart disease, diabetes, and stroke. Heterogeneous Stock (HS) Rats are an outbred population based model used in previous gene by environment studies due to their phenotypic diversity. In this study, three different inbred founders of the HS rat strain (ACI, BN, MR) were used. It is hypothesized that chronic PFOS exposure will alter the risk of metabolic disease and endocrine disruption in HS founder rats. The rats were given a control diet or a diet containing 30mg/kg of PFOS; measures of body weight and body composition through Nuclear Magnetic Resonance (NMR) were performed, along with glucose tolerance, lipids measurements, and tissue collection at euthanasia. Males and females exposed to PFOS in all three strains, showed a decrease in body weight compared to the control group. The results from NMR showed no significant values across the strains or the sexes. The triglyceride values showed a decrease in the MR strain of 65% in females and 118% in males. Furthermore, there was an increase in the liver size for the PFOS group across the three strains for both sexes. Finally, for females, there was a decrease in thyroid for the PFOS group in ACI of 46%, and an increase in adrenal glands for the BN of 9%. Similarly, this increase was observed for the male BN at 49%. These results suggest that chronic exposure of PFOS induced endocrine dysfunction and liver intoxication. Further analysis of other tissues collected, and measurements of triglycerides stored in the liver is intended for future studies. Due to these evident metabolic effects in the three HS founders studied, it is warranted to repeat this study in the future using HS rats to find possible genetic effects.

Analysis of Sodium Intake Patterns in Mice Using an Automated Home-Cage Sipper Device

Background: An excessive amount of sodium intake leads to an increased risk of cardiovascular disease. β -arrestin-2 (*Arrb2*) is a cytoplasmic protein that mediates and modulates second-messenger signaling by various G protein coupled receptors. Mutations in this gene are associated with cardiovascular disease. Recently our team has shown that *Arrb2* plays a key role in controlling sodium intake behaviors.

Current technologies available in our lab permit measures of drink volumes consumed per day, however, the patterns of these drinking choices cannot be further studied in the home cage. We hypothesize that use of a new open-source, automated drink sipper analysis system will permit us to analyze the patterns of fluid intake in mice. Characterizing the number, volume, and circadian distribution of saline drinking bouts of control mice and *Arrb2*-KO mice will help us to better understand the biology controlling sodium intake.

Methods: Using an open-source document, a 3-D model was printed. The code from the open source was edited to record each time a photobeam was broken in either the right or left state and when the photobeam returned to its unbroken state. The devices were placed in the home cages of control (n=4) and *Arrb2*-KO (n=2) mice and observed every 24 hours for a four-day period.

Results: These automated sipper devices permitted mapping of drinking bouts throughout the light and dark cycles. Although the small sample size for the *Arrb2*-KO mice precludes formal statistical analyses, initial trends hint that the animals had no problems consuming liquids from the device, and expected trends were confirmed. In addition, the intake of 0.15 mol/L sodium chloride in the *Arrb2*-KO mice occurred both in the dark and light phase, which could be due to an increased motivation to consume saline even during the light phase. Technical issues and ideas for improvement of the device and software were documented, and ongoing work is focused on improvement of both the hardware and software as we begin to use the devices in additional studies of live animals.

Conclusion: Use of an automated two sipper device will enable our team to perform more sophisticated dissection of saline intake behaviors, supporting our ongoing dissection of the biology that controls sodium ingestive behaviors. Future work is simultaneously aimed at (i) additional technical improvements of the devices, and (ii) use of these systems to map drinking bout microstructures toward various drink types in animal models under study by our team.

Courtney Griffin-Howard University
[Aprill Z. Dawson, PhD, MPH; Joni S. Willians, MD, MPH]
[MCW Center for Advancing Population Science]

Effective Clinical Trial Recruitment Strategies For Racial/Ethnic Minorities With Type 2 Diabetes

Approximately 537 million adults worldwide have diabetes. In the US, racial and ethnic minority groups are disproportionately affected by diabetes. Studies are needed to identify effective strategies for improving glycemic control and other diabetes-related outcomes for disparate populations. Therefore the aim of this project was to summarize the literature on effective strategies for recruiting racial/ethnic minorities with type 2 diabetes into clinical trials within the United States. By using databases such as PubMed and the Cochrane Systematic Review, we were able to locate 8 articles that categorized recruitment strategies into four primary categories: Provider Referrals and Electronic Medical Records (EMRs); Phone Calls and Mailings; Social Media; and Community Engagement. Out of 939 participants in U.S. clinical trials, 77% were recruited using community engagement. A total of 5,384 participants in the clinical trials used EMR and provider referrals as a strategy for recruitment. From those participants, 4,217 participants (84%) were enrolled in the study using this strategy. In summary, the most common method of recruitment was electronic query to identify eligible participants followed by community engagement.

Key Words: Type 2 Diabetes, Minorities, Recruitment Strategies

Zainab Khan – Marquette University
Joseph Carroll, PhD
MCW Department of Ophthalmology and Visual Sciences

Exploring potential bias within adaptive optics-corrected visual acuity (AO-VA) thresholds in individuals with normal vision

Background: Vision loss affects over 1.1 billion people globally, and people with vision loss often have an increased risk for health conditions like dementia and cardiovascular disease (*The International Agency for the Prevention of Blindness*, 2022). Understanding retinal structure and function is crucial to developing therapies for and preventing vision loss. Vision is initiated in the retina where photoreceptors (cones and rods) convert light into signals the brain can interpret. Adaptive optics scanning light ophthalmoscopy (AOSLO) enables high-resolution imaging of individual retinal cells and facilitates the study of retinal structure and function at a single-cell level. Here we investigated differences in visual acuity measurements obtained through AO-VA versus an individual's predicted visual acuity derived from the minimum spacing of their cone photoreceptor mosaic. Prior studies using AO-VA have shown a disagreement between observed and predicted acuity values. We hypothesize that human response biases during psychophysical testing may contribute to this disagreement.

Methods: To identify biases in AO-VA testing methods that affect observed versus predicted visual acuity in healthy controls, several methods were used. First, we analyzed past AO-VA data from thirteen subjects to assess whether they had a bias in response direction. Previous tests of ten subjects were also analyzed to evaluate whether there were any biases in the presented stimulus orientation. To further explore directional selection bias, an experiment to see how subjects would respond to a non-directional stimulus (XX pixel, subthreshold cross) was designed by altering previous MATLAB scripts. Three subjects completed an augmented four-alternative forced-choice task with AO-VA to assess response bias. During this testing, subjects were shown ~15 trial blocks and 30 directional stimuli (E's) and 10 non-directional cross stimuli per trial block. The stimulus size varied to assess the subjects' visual acuity, and both stimuli were shown for 0.5 seconds. Subject responses were recorded and analyzed to assess if any had a response bias. The subjects' data was plotted in both the horizontal and vertical stimulus direction for easier analysis.

Results: Psychophysical testing revealed unexpected differences between the thirteen subjects whose response data was retrospectively analyzed – when subjects answered incorrectly, they had an average horizontal bias 41% of the time and a vertical bias 20% of the time where they answered in the same plane but opposite direction of the stimulus. Analyzing previous data of ten subjects revealed that the E stimulus shows up in the horizontal plane 53% of the time and in the vertical plane 47% of the time. The E stimulus does not appear to drive bias as it shows up approximately evenly in both planes. After adding the cross, we found that not all subjects have strong bias. When shown a cross, the three subjects answered in the horizontal plane 75%, 45%, and 51% of the time, respectively.

Conclusions: This study revealed that biases in psychophysical testing methods, specifically forced-choice orientation tests, can affect the accuracy of AO-VA measurements. The data show that subject-specific biases, rather than the stimulus orientation itself, contributes to discrepancies between observed and predicted visual acuity. This underscores the importance of considering individual response biases when interpreting AO-VA results. To improve the reliability of these measurements, it is essential to account for such biases in future psychophysical testing. Better understanding and mitigating these biases will enhance visual acuity test accuracy and can help improve the efficacy of emerging interventions for retinal diseases.

Keywords: Adaptive Optics Scanning Light Ophthalmoscopy, Photoreceptors, Psychophysics, Adaptive Optics Visual Acuity

Vivien Blecking – University of Wisconsin-Milwaukee

Olena Isaeva, PhD

MCW Department of Cell Biology, Neurobiology, and Anatomy

The effect of chemotherapy treatment on pain-related behaviors of adult and elderly mice

Background

Chemotherapy-induced peripheral neuropathy (CIPN) is the most common side effect of Paclitaxel, a drug used to treat various types of cancer. CIPN causes pain, tingling, or numbness in the hands and feet during or after Paclitaxel treatment. Over 65% of cancer survivors are over 65, but older adults are often excluded from research. Previous studies show that elderly cancer patients report less pain and interference with daily activities yet have worse mechanical and thermal sensations than middle-aged patients. While changes in mechanical sensitivity in young and adult rodents after chemotherapy have been established, the effects of chemotherapy on pain-related behaviors in elderly mice remain unexplored. This study examines involuntary and voluntary pain-related behavioral responses in adult and elderly mice after Paclitaxel treatment.

Methods

Adult (7-8 months) and elderly (24 months old) male mice received two intraperitoneal injections of Paclitaxel (0.8 mg/kg) with 48 hours between injections. Pain-related behavior was assessed before injections and 1-3 days after the last injection. Involuntary behavioral responses to mechanical sensitivity were tested by observing the mice's reflexive responses to light and noxious stimuli applied to the paw. Voluntary behavioral responses were tested using a Conflict Avoidance Assay (CAA), where mice were placed in a chamber with an aversive bright light. To escape the light, the mice had to cross a long corridor with either smooth flooring or noxious probes to enter a dark chamber. Escape latency from the light chamber, and time spent in the tunnel were recorded to evaluate how spontaneous pain influences decision-making.

Results

We found that elderly mice are more mechanically sensitive to noxious stimuli than adult mice both at baseline and after Paclitaxel treatment. Additionally, elderly mice showed increased sensitization to light touch stimuli after Paclitaxel treatment. Both adult and elderly mice exhibited decreased escape latency and time spent in the tunnel with smooth, innocuous flooring. However, only adult mice showed enhanced pain-avoidance behavior after Paclitaxel treatment.

Conclusion

This study shows that elderly mice exhibit greater mechanical hypersensitivity but less motivation to avoid noxious stimuli compared to adult mice, highlighting age-related differences in pain perception and pain-avoidance behavior after chemotherapy treatment.

Juliet Peterka, DePaul University
Mallika Khurana, MS, Pui-Ying Lam, PhD
MCW Department of Cell Biology, Neurobiology, and Anatomy

Developing a looming response vision assay to assess CNS regeneration in adult *Danionella cerebrum*

Background

Danionella cerebrum is an emerging fish model for neurobiology. *D. cerebrum* remain small and transparent in the central nervous system (CNS) through adulthood, so they are particularly useful for longitudinal live imaging (Schulze, 2018, Lam, 2022). Data from our lab has shown that adult *D. cerebrum* regenerate their retinal ganglion cell (RGC) axons after an optic nerve crush (ONC) (unpublished). However, the functionality of the regenerated RGC axons is unclear. Here, we establish a behavioral assay for assessing *D. cerebrum* vision in which a virtual looming “predator-like” stimulus causes a startle response. The effects of looming stimuli on *D. cerebrum* were previously unknown.

Methods

We created multiple types of looming stimuli in which a black circle grew on a white screen. These videos were presented to the fish on a monitor centered above the tank, and swimming behavior was tracked using AnyMaze (Stoelting Co., Version 7.4). To optimize the assay, different circle sizes and circle growth rates were tested. Circle size was quantified as angular size, i.e. the size of the angle formed by the perimeter of the circle at the fish’s eye, and circle growth rate was quantified as the expansion rate of the circle’s radius in cm/s.

Results

Swimming speed increased in response to 33-84° stimuli (radius = 1.78-5.4 cm) but not to 9-18° stimuli (radius = 0.47-0.96 cm). All tested circle growth rates (1.0-21.6 cm/s) caused an increase in post-stimulus swimming speed. The most consistent and substantial change in speed was observed in response to the 84° looming stimulus with a growth rate of 5.4 cm/s. When comparing average fish speed over two seconds before and after the stimulus, this stimulus was observed to cause an 11-fold increase in swimming speed ($n=6$).

Conclusion

We developed and optimized a behavioral assay to assess the vision of adult *D. cerebrum*. This assay will be applied to ONC fish to assess the functionality of their regenerated RGC axons. This will help validate *D. cerebrum* as a model for CNS regeneration and could aid vision regeneration research.

References

Lam, Pui-Ying. (2022) Disease Models & Mechanisms 15, 049753. 10.1242/dmm.049753.
Schulze, Lisanne et al. (2018) Nature Methods 15, 977-983. 10.1038/s41592-018-0144-6.

Mae Jones – University of Michigan
Elena Semina, PhD and Samuel Thompson, BS
MCW Department of Pediatrics, MCW Department of Ophthalmology and
Visual Sciences

Investigating the Roles of ARHGAP18 and PRR12 in the Development of Microphthalmia

Background

Microphthalmia is an ocular condition where the eye is greater than two standard deviations smaller in axial length as compared to the mean length based on age. Resulting from disruptions to eye development between 4 and 8 weeks of age, it is frequently associated with anophthalmia (absence of eye) and coloboma (lack of optic fissure closure). Diagnostic rates for microphthalmia, anophthalmia, and coloboma (MAC) are only 15-30%. PRR12 and ARHGAP18 have been previously identified as possible genes associated with MAC from patient data. In this study, we looked to further explore this association by breeding variants in orthologous zebrafish genes (*prr12a* and *arhgap18*) and observing for similar phenotypes. We hypothesized that zebrafish homozygous for variants of *arhgap18* or *prr12a* could develop phenotypes on the MAC spectrum, particularly microphthalmia.

Method

ZIRC zebrafish lines containing the variants in *arhgap18* and *prr12a* were fin clipped, and DNA was extracted using 50 mM NaOH. Both genes underwent polymerase chain reaction (PCR) and gel electrophoresis to confirm DNA amplification. PCR products were sequenced, and heterozygous individuals were identified. Heterozygous fish were bred, and embryos were cleaned before being placed in 1-phenyl 2-thiourea (PTU) solution. Embryos were incubated and dechorionated between 24 and 48 hours post fertilization (hpf). At 48 hpf, embryos were lined up and compared to observe for phenotypes. Embryos showing phenotypes were separated. At 6 days post fertilization, embryos were imaged from a lateral and dorsal angle using a microscope (at 27x, 60x, 110x, and 168x magnification). DNA was extracted and amplified using the procedure stated above before being sent for sequencing.

Results

A hooked tail phenotype was observed in approximately 25% of the *prr12a* embryos. The phenotype displayed high variation from a slight bend at the end of the tail to complete malformation of the entire tail. Genotypes have not yet been obtained. In multiple clutches of *arhgap18* embryos, small eyes were observed in less than 25% of embryos. Sequencing data showed that, in the phenotype positive group, 12 of 29 embryos were homozygous for the variant, 16 of 29 embryos were heterozygous, and 1 embryo was wild type. On the other hand, in the phenotype negative group, 1 of 16 was homozygous for the variant, 7 of 16 were heterozygous, and 8 of 16 were wild type.

Conclusion

While phenotypes were present after breeding fish with variants in *prr12a* and *arhgap18*, no conclusions can yet be made about any associations between the variants and the phenotypes. Future research will look to find the genotypes for *prr12a* embryos with tail phenotypes, as well as explore possible explanations for the small eyes of many heterozygous *arhgap18* embryos. Deciphering these relationships could possibly help provide molecular diagnoses for more patients with MAC phenotypes.

Fewer sources of platelet derived growth factor-BB found in *Danio rerio pak2a* mutants

Background

Intraventricular hemorrhages (IVH) are the result of blood spilling from the brain blood vessels, through the matrix, and into the ventricles. IVH typically occurs in premature babies because of the fragility and underdeveloped blood vessels in the brain. Pericytes and endothelial cells are major contributors to the stability of blood vessels. Endothelial cells secrete a ligand called platelet derived growth factor subunit B (PDGF-BB), that binds to the PDGF- Beta receptor on the surface of pericytes, and this interaction triggers signals that facilitate vascular stability. Endothelial cells also contain heparan sulfate proteoglycans (HSPG) that interact with matrix proteins and act as co-receptors of PDGF-BB. A mutation in the *p21-activated kinase 2a (pak2a)* gene in zebrafish leads to unstable blood vessels and brain bleeding. Thus, *pak2a* may serve as a model of IVH. We hypothesize that in *pak2a* mutants there will be less PDGF-BB and HSPG around the major blood vessels compared to wild type.

Methods

To investigate the hypothesis, we used 52 hours post fertilization *pak2a* mutant zebrafish to understand the interactions of PDGF-BB and HSPG, and their effect on blood vessel stability in the brain. Our approach to test this hypothesis included immunofluorescence, microscopy, and qPCR. The embryos were observed using a Keyence microscope, and sources of PDGF-BB near the major blood vessels were quantified using the Keyence BZ-X Analyzer.

Results

Our results suggest that less PDGF-BB is present in *pak2a* mutants around the major blood vessels compared to wild type *pak2a* zebrafish. Our preliminary conclusion is that fewer sources of PDGF-BB result in less stable blood vessels because of the lack of interaction between the ligand and receptor which may lead to bleeding.

Conclusion

Future studies include using qPCR to compare the expression of genes in PDGF-BB and HSPG biosynthesis in wild type and *pak2a* mutants and staining for the presence of HSPG with antibodies. Understanding secretion of PDGF-BB and its interaction with HSPG are key to the mechanistic understandings of IVH.

Keywords: *pak2a*, platelet derived growth factors, heparan sulfate proteoglycans, intraventricular hemorrhages